AIAA 80-1676R

A New Method for Optimizing Multiple-Flyby Trajectories

L.A. D'Amario,* D.V. Byrnes,† and R.H. Stanford‡
Jet Propulsion Laboratory, California Institute of Technology, Pasadena, Calif.

A new procedure has been developed which minimizes total impulsive ΔV for multiple-flyby trajectories with constraints on flyby parameters and maneuver times. The method involves solving a bounds-constrained parameter optimization problem with a Newton algorithm utilizing analytic first and second derivatives. Each trajectory segment connecting consecutive maneuver points is found by first targeting from the preceding maneuver point to the parameters of the upcoming flyby and then propagating the resulting trajectory to the next maneuver point. Multiconic techniques are used for trajectory propagation and computation of the state transition matrix. This procedure has successfully optimized Galileo satellite tours containing up to eleven flybys.

I. Introduction

In recent years mission analysis has become increasingly concerned with trajectories containing one or more gravity-assist flybys. Multiple planetary flyby trajectories have already appeared in the Mariner-Venus-Mercury[1] and Voyager[2] missions, and the interplanetary phase of the Galileo mission once involved a powered Mars flyby to reach Jupiter.[3] Multiple flyby trajectories also appear in missions containing satellite tours such as Galileo[4] and the proposed Saturn orbiter mission,[5] and a mission being studied to explore the Earth's geomagnetic tail involves repeated close flybys of the moon.[6]

Multiple-flyby trajectories, which are very difficult to generate using traditional methods, are typically constructed in segments, usually with no more than one flyby per segment. These trajectories may, therefore, require velocity impulses, or maneuvers, at the breakpoints. For the Voyager mission, ballistic (zero ΔV) multiple flyby trajectories can be found. In the case of the Galileo satellite tour, relatively small ΔV's (several meters per second) are needed. For Galileo interplanetary trajectories, extremely large ΔV's (up to 1 km/s) are presently required to alter the flight path. Minimizing the total ΔV required for multiple flyby trajectories is important because it relates to minimal total fuel requirements, as well as providing a method for finding ballistic trajectories in a manner which avoids the numerical problems associated with simple targeting schemes.

The multiple flyby optimization problem is considerably complicated by the need to constrain variables such as maneuver times and flyby parameters. These constraints arise from scientific objectives or mission operations limitations. The constraints are usually expressed as range constraints, i.e., an upper and lower limit are given for the constrained variable. If the upper and lower limits are the same, the range constraint becomes an equality constraint.

A method for solving this problem as a parameter optimization problem was recently developed by the authors.[7] This method utilized the times and positions of the maneuvers as parameters, or independent variables, for the optimization, and a quasi-Newton algorithm (using only first-derivative information) to search for the minimum ΔV. There were, however, several drawbacks to this method: constraints were handled by means of penalty functions; the computing time required to generate a solution was excessive, primarily because terminal convergence was exceedingly slow; and, occasionally, trajectory segments could not be fit between maneuver points because of numerical targeting problems.

A quite different formulation for the solution of the multiple flyby optimization problem has been developed and is described in this paper. This new method has eliminated the drawbacks of the method in Ref. 7. In the new method, the independent variables are the altitudes, B-plane angles (defined in Sec. II), and periapse times of each flyby, along with the maneuver times. Any of these variables may be constrained.

Allowing any of the independent variables to be constrained by the use of simple range constraints eliminates the need for penalty functions. Range constraints on independent variables are handled very easily by the optimization algorithm. The choice of independent variables in this new method has also contributed to reducing, by about an order of magnitude, the amount of computing time required to optimize the trajectory. This is due to the use of a much simpler trajectory targeting scheme, which has also essentially eliminated the earlier numerical targeting problems.

In this new formulation of the multiple flyby optimization problem, the cost function is defined as the weighted sum of the squares of the magnitudes of all the ΔV's, instead of the sum of the magnitudes themselves as in Ref. 7. This sum-of-squares cost function has several advantages. It eliminates discontinuities in the cost gradient which occur for the sum-of-magnitudes cost function whenever any ΔV approaches zero. Also, a good approximation to the second-derivative (Hessian) matrix can be computed using only the first derivatives of the velocity vectors. This has allowed the use of a Newton optimization algorithm, which has resulted in a spectacular improvement in terminal convergence and computing time.

In order to generate the sum-of-magnitudes solution while retaining the advantages of the sum-of-squares cost function, each ΔV in the cost function is weighted. The optimization method can automatically compute new weights which are inversely proportional to the magnitudes of the ΔV's, and then restart the optimization using the new weights. After several restarts of a few iterations each, the desired sum-of-magnitudes solution is easily found.

The optimization procedure has been implemented with two different models of multibody dynamics, both based on multiconic theory. One version uses a three-body model and a one-step multiconic propagation method. The other version uses a multistep, multiconic method which accounts for the central body, an arbitrary number of satellites, solar perturbations, and central-body oblateness.

Presented as Paper 80-1676 at the AIAA/AAS Astrodynamics Conference, Danvers, Mass., Aug. 11-13, 1980; submitted Sept. 16, 1980.

*Member Technical Staff. Member AIAA.
†Consultant.
‡Member Technical Staff. Member AIAA.

II. Parameter Optimization Problem

The multiple flyby trajectory optimization problem is solved as a parameter optimization problem. The solution method is summarized as follows. On each iteration of the optimization procedure, a complete end-to-end trajectory is generated. The complete trajectory is divided into segments (see Fig. 1), and each segment, which contains one flyby, is determined as explained in Sec. III. There is, in general, a velocity mismatch at each breakpoint, or maneuver point, and the combination of these impulsive ΔV's defines the cost function for the optimization. The optimization problem is solved by varying the independent variables within their allowable ranges, such that the total cost is minimized. The set of independent variables consists of the altitudes, B-plane angles, and periapse times of the flybys, along with the maneuver times. The B-plane angle unambiguously defines the orientation of the approach hyperbola. Figure 2 indicates this angle as θ. The B-plane is oriented perpendicular to the incoming asymptote and passes through the center of the body.

A. Optimization Formulation

The cost function F is defined as the weighted sum of the squares of the magnitudes of all of the maneuver ΔV's. This quadratic form is in contrast to the sum of the magnitudes used in Ref. 7. The cost function is given by

$$F=\sum_{i=0}^{n-1} f_i \Delta\bar{V}_i^T \Delta\bar{V}_i \tag{1}$$

where the f_i are weight factors for each of the n maneuvers, and the $\Delta\bar{V}_i$ are the three-vector velocity differences at each maneuver point. Taking partial derivatives of Eq. (1) with respect to the m-independent variables $\bar{X}$, gives the gradient vector $\bar{g}$ (an m-vector) and the Hessian matrix H (an $m\times m$ matrix) as

$$\bar{g}^T=\frac{\partial F}{\partial \bar{X}}=2\sum_{i=0}^{n-1} f_i \Delta\bar{V}_i^T \frac{\partial \Delta\bar{V}_i}{\partial \bar{X}} \tag{2}$$

and

$$H=\frac{\partial^2 F}{\partial \bar{X}^2}=2\sum_{i=0}^{n-1} f_i \Delta\bar{V}_i^T \frac{\partial^2 \Delta\bar{V}_i}{\partial \bar{X}^2}+2\sum_{i=0}^{n-1} f_i \left(\frac{\partial \Delta\bar{V}_i}{\partial \bar{X}}\right)^T \left(\frac{\partial \Delta\bar{V}_i}{\partial \bar{X}}\right) \tag{3}$$

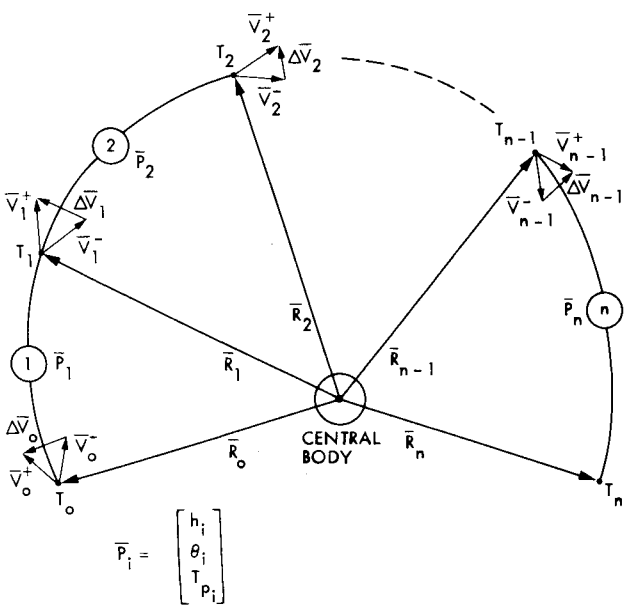

Fig. 1 Multiple flyby trajectory schematic.

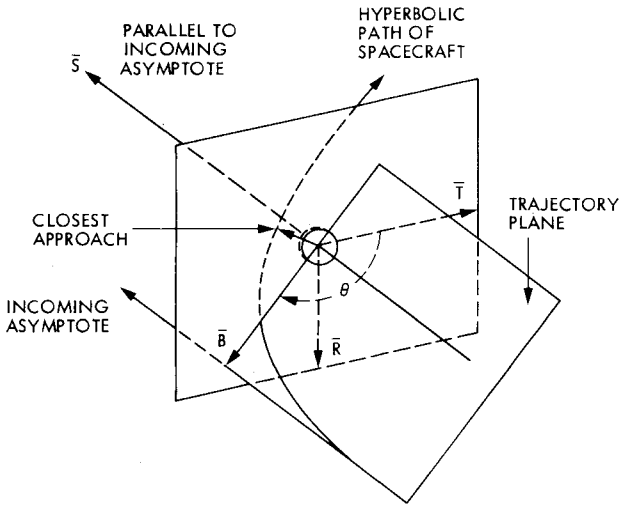

Fig. 2 B-plane coordinate system.

where

$$\bar{X}=\begin{bmatrix} \bar{P}_1 \\ T_1 \\ \bar{P}_2 \\ T_2 \\ \cdot \\ \cdot \\ \cdot \\ \bar{P}_n \end{bmatrix} \tag{4}$$

and where

$$\bar{P}_i=\begin{bmatrix} h_i \\ \theta_i \\ T_{p_i} \end{bmatrix} \tag{5}$$

are the flyby altitude, B-plane angle, and periapse time for the ith flyby. Notice that in Eq. (2) the gradient is smooth and well behaved even if any of the $\Delta\bar{V}_i$'s approach zero. This is in contrast to the sum-of-magnitudes formulation of Ref. 7 where the gradient has a discontinuity when any $\Delta\bar{V}_i$ becomes zero.

The expression for H in Eq. (3) consists of two terms, only the first of which requires second-derivative information. In numerical tests the $\Delta\bar{V}_i$ are observed to be quite linear functions of the independent variables, so the quantity $\partial^2\Delta\bar{V}_i/\partial\bar{X}^2$ is small in an absolute sense. Also, near a solution the $\Delta\bar{V}_i$'s become quite small. For these reasons the first term of H is much smaller than the second, permitting H to be approximated to a high degree of accuracy with only first-derivative information.

Having both the Hessian and the gradient available allows the use of a Newton optimization algorithm, with resulting quadratic convergence near a solution. The Newton algorithm is based on expanding the cost function F in a Taylor series about the nominal or starting value of the vector of independent variables $\bar{X}_0$. Thus,

$$F=F_0+\bar{g}_0^T(\bar{X}-\bar{X}_0)+\tfrac{1}{2}(\bar{X}-\bar{X}_0)^T H_0(\bar{X}-\bar{X}_0)+\cdots \tag{6}$$

The corresponding expansion for the gradient $\bar{g}$ is

$$\bar{g}=\bar{g}_0+H_0(\bar{X}-\bar{X}_0)+\cdots \tag{7}$$

Assuming that H_0 is positive definite, the minimum of F occurs when $\bar{g}$ is zero. Approximating F as a quadratic gives the solution as

$$\bar{X} = \bar{X}_0 - H_0^{-1}\bar{g}_0 \tag{8}$$

Since H_0 is the matrix of second partial derivatives, it is a symmetric matrix.

The modified Newton algorithm uses the step defined by Eq. (8) as a trial step, and then performs a one-dimensional line search in that direction. The result of that search becomes the starting value $\bar{X}_0$ for the next iteration. The process continues until a satisfactory solution is obtained.

Any or all of the independent variables may be bounded by range constraints. During a line search, an independent variable may reach one of its limits, in which case it is fixed at that limit and the optimization continues on the reduced subset. When a minimum on a subset is reached, any or all of the bound variables may be freed if a lower minimum is indicated.

An algorithm developed at the National Physical Laboratory of England based on the material in Chap. 2 of Ref. 8 is used in our method with some modification. Use of this modified Newton algorithm has resulted in a spectacular improvement in convergence and computation time when compared with the quasi-Newton method used in Ref. 7.

B. Weight Factors

The cost function defined in Eq. (1) is the weighted sum of the squares of the magnitudes of the $\Delta\bar{V}_i$. The desired solution, however, is the minimum of the sum of the magnitudes of the $\Delta\bar{V}_i$. If the weight factors f_i used in Eq. (1) could be set to

$$f_i = 1/|\Delta\bar{V}_i^*| \tag{9}$$

where the $\Delta\bar{V}_i^*$ correspond to the sum-of-magnitudes solution, then the weighted sum-of-squares solution is seen to be equivalent to the sum-of-magnitudes solution. In practice, after a solution is found, the optimization is restarted with new weights computed from the $\Delta\bar{V}_i$ of that solution. With several restarts of a few iterations each, the desired sum-of-magnitudes solution is easily found. Use of this weighting scheme generates the sum-of-magnitudes solution while retaining all of the advantages of the sum-of-squares formulation. Section IV discusses in detail the important differences between the two solutions.

C. Partial Derivatives

Fundamental to the optimization method described above is the computation of the $\Delta\bar{V}_i$ used in the cost function F and the partial derivatives $\partial\Delta\bar{V}_i/\partial\bar{X}$ used in the gradient and the Hessian. Referring to Fig. 1, it is seen that the $\Delta\bar{V}_i$ are simply the velocity discontinuities at each maneuver point, with the arrival and departure velocities at that point determined by the process described in Sec. III. The partial derivatives must relate the variation of each $\Delta\bar{V}_i$ with respect to each component of $\bar{X}$. These derivatives depend only on the state transition matrices of the various trajectory segments and the local Jacobians relating periapse state to the altitudes, B-plane angles, and periapse times for each flyby. The process of finding the expressions for the derivatives although straightforward in concept is, in fact, a very lengthy, tedious process requiring repeated application of the chain rule after very careful definition of the dependencies of each variable. A summary of the partial derivatives is given in the Appendix, showing their cascading nature, whereby each $\Delta\bar{V}_i$ depends on every independent variable preceding it as well as the three periapse parameters immediately following it, but nothing else.

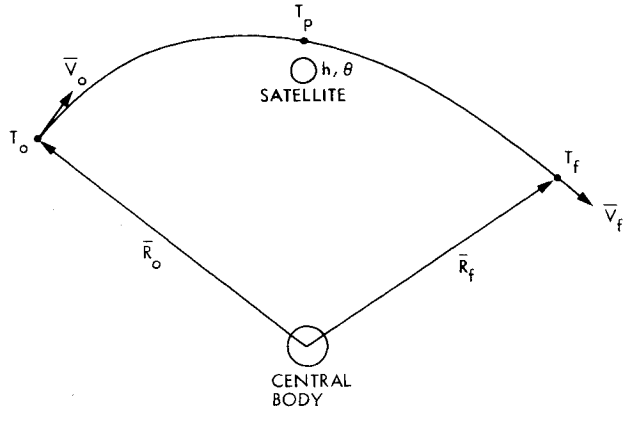

Fig. 3 Satellite flyby trajectory.

III. Trajectory Generation

During the solution to the parameter optimization problem, each evaluation of the cost function requires the generation of a complete trajectory. A schematic of the complete trajectory is shown in Fig. 1. The complete trajectory is generated segment by segment beginning with the first and proceeding to the last. Each trajectory segment contains precisely one flyby.

Each segment of the trajectory shown in Fig. 1 is generated in two steps. Figure 3 shows one segment of the trajectory. In the first step, the trajectory is targeted from the position $\bar{R}_0$ and time T_0 of the preceding maneuver to a set of satellite flyby conditions. These flyby conditions are the altitude h, B-plane angle θ, and periapse time T_p. The three components of the initial velocity $\bar{V}_0$ are varied to satisfy the three satellite periapse conditions. In the second step, this trajectory is propagated from T_p to the time of the next maneuver, T_f.

The flyby targeting problem is solved using an ordinary Newton iteration scheme, which is described as follows:

1) Propagate a trajectory forward from the fixed time T_0 and fixed position $\bar{R}_0$ with a guessed velocity $\bar{V}_0$ to the satellite periapsis at time T_p', which, in general, is not equal to T_p, the desired periapse time. The satellite-relative periapse state (position and velocity) at T_p' is $\bar{X}_p$.

2) Calculate the error, $\Delta\bar{P}$, in the periapse target variables, where

$$\bar{P} = \begin{bmatrix} h \\ \theta \\ T_p \end{bmatrix} \tag{10}$$

3) Determine the correction to the initial velocity $\bar{V}_0$ from

$$\Delta\bar{V}_0 = K^{-1}\Delta\bar{P} \tag{11}$$

where K is defined by

$$K = \frac{\partial\bar{P}}{\partial\bar{X}_p}\frac{\partial\bar{X}_p}{\partial\bar{V}_0} \tag{12}$$

The quantity $\partial\bar{P}/\partial\bar{X}_p$ (a 3×6 matrix) is the local Jacobian at T_p', relating the target variables to the periapse state. The quantity $\partial\bar{X}_p/\partial\bar{V}_0$ (a 6×3 matrix) relatesthe change in the periapse state to a change in $\bar{V}_0$, and is obtained from the state transition matrix for the trajectory from T_0 to T_p'.

4) Update the initial velocity, $\bar{V}_0$, and repeat steps 1-3 until $\Delta\bar{P}$ is below a given tolerance.

Two methods for propagating the trajectories are available to the optimization procedure. One method, called the 1STEP method, uses a three-body dynamic model (central body, flyby satellite, and spacecraft) and a one-step multiconic propagation technique. The 1STEP method was developed by Byrnes[9] and is based on the pseudostate theory of Wilson.[10] This method provides an excellent approximation to the true

three-body trajectory and eliminates 80-90% of the error of simple conic methods. The other trajectory propagation method, called the MULCON method, uses a multistep, multiconic technique which models the central body, an arbitrary number of satellites, solar perturbations, and central-body oblateness. The MULCON method is based on the work of Kwok and Nacozy,[11] which was derived from several sources.[10,12-14] This method produces trajectories with accuracies approaching that of precision numerical integration for significantly less computational effort. Multiconic techniques are especially well-suited to the generation of trajectories in the current application because the state transition matrix on each trajectory propagation is calculated analytically without significant additional computational effort.

Since the 1STEP method is computationally fast and low cost, it is particularly useful for preliminary design and tradeoff studies which only require the basic characteristics of the optimized solution. The solution produced using the 1STEP method provides good initial inputs for the MULCON method, which is at least an order of magnitude slower and more expensive. The MULCON method is used when a solution with more precise dynamic modeling is desired.

IV. Results

The optimization procedure described in this paper has been coded in Fortran V on a Univac 1100/81 computer at the Jet Propulsion Laboratory. There are two versions of the computer program, corresponding to the 1STEP and MULCON trajectory models. The two versions differ only with respect to the trajectory generation subroutines; all other software is the same.

In order to illustrate the capabilities and performance of the optimization procedure, results are presented of the analysis of a ten flyby Galileo satellite tour.[4] This tour has a duration of 15 months and includes one Callisto, five Ganymede, and four Europa encounters. It contains close as well as distant flybys with near-polar and equatorial orientations.

The starting conditions of this tour are a fixed time and position near apojove of the first orbit about Jupiter, prior to the first satellite flyby. The tour ends near apojove of the eleventh orbit, after the tenth flyby. All satellite encounters occur near perijove.

Table 1 shows the sequence of flybys in the tour. In the flyby designation, C, G, and E denote Callisto, Ganymede, and Europa, respectively, and the number represents the sequential ordering of the flybys. Also included in this table are the upper and lower limits of the range constraints on altitude and B-plane angle used during the optimization. These limits are determined by mission operations constraints and scientific objectives.

Initial conditions for altitudes, B-plane angles, and periapse times of each flyby and for maneuver times are obtained from a conic satellite tour design program which does not have an optimization capability. The initial conditions for maneuver times correspond to apojove of each orbit.

Table 1 Satellite tour trajectory flyby sequence and constraints

	Altitude limits, km		B-plane angle limits, deg	
Flyby	Lower	Upper	Lower	Upper
G1	750	1500	90	180
G2	500	1500	90	180
G3	20,000	70,000	−90	90
C4	200	1500	−20	20
E5	200	1500	75	105
E6	200	1500	−70	−20
G7	15,000	30,000	0	40
E8	200	6000	−20	20
E9	15,000	60,000	−90	90
G10	200	4000	−20	20

A. 1STEP Analysis

The 1STEP analysis was performed in a single computer run consisting of four stages. During each stage certain independent variables are fixed (deactivated) by means of an equality constraint. The four stages of the optimization are:

1) Generate the sum-of-squares solution with the flyby variables (h, θ, T_p) active and the maneuver times (T) fixed at their initial values.

2) Generate the sum-of-magnitudes solution using the weight factors described in Sec. II. The maneuver times remain fixed.

3) Fix the flyby variables at the solution from stage 2 and continue the optimization with selected maneuver times activated.

4) Fix the maneuver times at the solution from stage 3 and continue the optimization with the flyby variables reactivated.

Experience with analysis of several satellite tours has shown that it is more efficient to separate the activation of flyby variables and maneuver times. The range constraints on altitude and B-plane angle applicable when those variables are active are given in Table 1. Any given maneuver time, when active, is constrained by mission operations limitations to a lower limit of three days after the previous satellite flyby and an upper limit of three days before the next flyby.

The results of the 1STEP optimization, compared to the conic results, are presented in Tables 2-4. Table 2 lists the ΔV for each maneuver and the total ΔV for the solutions at each stage of the optimization. Tables 3 and 4 list the altitudes and B-plane angles of each flyby. (The values for stage 3 are the same as those of stage 2, since the flyby variables were fixed during stage 3.) Those variables which are on a limit at a solution are marked.

Comparison of stage 1 (sum-of-squares solution) with stage 2 (sum-of-magnitudes solution) shows that several small ΔV's become zero. This behavior is a general characteristic of a sum-of-magnitudes solution. The net effect of the stage 2 optimization is a reduction of 5.1 m/s in total ΔV. Significant changes have occurred to several of the altitudes.

Table 2 Conic and 1STEP ΔV results

	ΔV, m/s				
	Conic	1STEP optimization stage			
Maneuver	analysis	1	2	3	4
1	1	0.8	0.7	0.7	0.7
2	7	0.4	0.3	0.3	0.4
3	5	0.6	0.3	0.3	0.1
4	0	1.4	0	0	0
5	22	14.8	15.1	15.1	15.6
6	0	1.5	0	0	0
7	0	1.9	0	0	0
8	13	18.4	22.7	22.1	0
9	26	16.3	11.9	8.7	15.5
Total	74	56.1	51.0	47.2	32.3

Table 3 Conic and 1STEP altitude results

	Altitude, km			
	Conic	1STEP optimization stage		
Flyby	analysis	1	2	4
G1	750	750[a]	1081	1142
G2	738	873	644	646
G3	54,002	70,000[a]	70,000[a]	70,000[a]
C4	1021	992	990	991
E5	900	200[a]	200[a]	200[a]
E6	145	200[a]	289	368
G7	18,109	22,061	22,071	21,781
E8	1730	5653	5485	5189
E9	28,001	60,000[a]	60,000[a]	60,000[a]
G10	2441	4000[a]	4000[a]	4000[a]

[a] This variable is on a limit (see Table 1).

Table 4 Conic and 1STEP *B*-plane angle results

	B-plane angle, deg			
	Conic	1STEP optimization stage		
Flyby	analysis	1	2	4
G1	125	130	134	135
G2	136	144	140	139
G3	0	−4	−5	−5
C4	−4	−5	−6	−7
E5	87	89	89	90
E6	−41	−56	−54	−52
G7	16	6	5	1
E8	1	−9	−15	−20[a]
E9	0	0	−1	−1
G10	−15	−20[a]	−20[a]	−20[a]

[a] This variable is on a limit (see Table 1).

Comparison of the stage 2 solution with the conic results shows a reduction of 23 m/s in total ΔV. Although there is a difference in dynamic modeling, the ΔV reduction is primarily due to optimization. The conic flyby parameters, which serve as initial conditions for the optimization, are quite different from the stage 2 solution. The general characteristics of the two, nevertheless, remain unchanged.

Notice that each large ΔV in the stage 2 solution is associated with an altitude or *B*-plane angle which is on a limit: ΔV_5 is associated with the h_5 limit; ΔV_8 is associated with the h_9 limit; and ΔV_9 is associated with the h_9, h_{10}, and θ_{10} limits.

The stage 3 solution is obtained by activating only the maneuver times for the three large maneuvers (T_5, T_8, and T_9) while fixing the flyby variables at their stage 2 values. The resulting changes in T_5, T_8, and T_9 were −0.001, −2.3, and −7.0 days, respectively. Referring to Table 2, the corresponding ΔV's decreased 0.0, 0.6, and 3.2 m/s for a net decrease of 3.8 m/s in total ΔV.

The stage 4 solution is obtained by reactivating the flyby variables and deactivating the maneuver times. An interesting result is that ΔV_8 decreases from 22.1 m/s to zero while ΔV_9 increases from 8.7 m/s to 15.5 m/s. The other ΔV's change only slightly and the net improvement is 14.9 m/s. To accomplish this, h_8, θ_7, and θ_8 changed significantly, and θ_8 is now at a limit. The fact that ΔV_8 has become zero implies that its maneuver time could now be placed anywhere on the ballistic portion of the trajectory between E8 and E9. The process of alternatively activating flyby variables and maneuver times can be carried on indefinitely, although the further ΔV savings to be obtained are quite small.

In every other satellite tour that has been investigated with this optimization procedure, it was found that no measurable total ΔV reduction occurred when the maneuver times were activated. It appears that for most satellite tours, the most efficient location to perform most maneuvers is near apojove where the velocity is smallest. Maneuvers which do not become zero in the optimization generally occur between opposite near-polar flybys of the same satellite.

B. MULCON Analysis

The analysis of this Galileo satellite tour is completed by application of the version of the optimization procedure with the MULCON trajectory model. Due to temporary core storage limitations associated with the JPL systems software operating on the UNIVAC 1100/81, the computer program with the MULCON trajectory model is limited to a maximum of four flybys. The trajectory must, therefore, be broken into four-flyby segments which are optimized separately, resulting in a suboptimal tour. For each four-flyby segment except the first, an initial ΔV at the junction point of the segments is included in the cost. This ΔV is referenced to the arrival velocity at that maneuver point from the optimization solution of the preceding four-flyby segment.

Table 5 ΔV results: 1STEP vs MULCON

	ΔV, m/s	
Maneuver	1STEP	MULCON
1	0.7	4.4
2	0.4	1.1[a]
3	0.1	1.8
4	0	1.0[a]
5	15.6	15.4
6	0	0.3[a]
7	0	2.0
8	0	0
9	15.5	18.0
Total	32.3	44.0

[a] Maneuver at junction point of four-flyby segments.

Table 6 Altitude and *B*-plane angle results: 1STEP vs MULCON

	Altitude, km		*B*-plane angle, deg	
Flyby	1STEP	MULCON	1STEP	MULCON
G1	1142	1024	135	133
G2	646	608	139	138
G3	70,000[a]	63,176	−5	−4
C4	991	974	−7	−4
E5	200[a]	200[a]	90	92
E6	368	200[a]	−52	−56
G7	21,781	28,112	1	6
E8	5189	5497	−20[a]	−11
E9	60,000[a]	60,000[a]	−1	−1
G10	4000[a]	4000[a]	−20[a]	−20[a]

[a] This variable is on a limit (see Table 1).

In optimizing a ten-flyby tour in four-flyby segments, one obvious choice for the segments is: 1-4, 5-8, 9-10. On the other hand, by selecting segments which overlap up to three flybys, a closer approximation to the true optimal tour can be obtained. The option chosen for this analysis was to overlap two flybys. This means that the complete tour is optimized in four segments: 1-4, 3-6, 5-8, 7-10.

The stage 4 1STEP solution supplies the initial conditions for the MULCON optimization. Since the MULCON and 1STEP trajectory models differ, the solutions will be different. Since there is only one close flyby on any trajectory leg, the three-body 1STEP model should account for most of the dynamics, except on the first few orbits where the period is still large and solar perturbations, not modeled in 1STEP, can be significant.

The 1STEP and MULCON solutions are given in Tables 5 and 6. The total ΔV for the MULCON solution is 11.7 m/s greater than that of the 1STEP solution. Part of this increase, particularly at the first maneuver, is a consequence of solar perturbations. In every tour that has been optimized with the 1STEP and MULCON trajectory models, solar perturbations have caused an increase in the first ΔV. The other reason for the increase in total ΔV is that the MULCON solution for the complete tour is a suboptimal solution, owing to the segmented optimization procedure. In particular, some of the zero ΔV's in the 1STEP solution are not zero in the MULCON solution, because they occur at a junction point between two four-flyby segments.

The results for altitude and *B*-plane angle in Table 6 show that the 1STEP and MULCON solutions are similar. The most significant differences are in the G7 and G8 flybys. These differences are probably associated with significant perturbations from other satellites included in the MULCON dynamics model, but not accounted for in the 1STEP dynamics model. In any case, the 1STEP solution was found to be an excellent starting guess for the MULCON optimization.

When the MULCON solution is used as a set of initial conditions for generation of a reference integrated trajec-

tory,§ it is found that the ΔV's agree to within a few tenths of meter per second. The altitudes and B-plane angles agree to within a few tenths of a kilometer and less than one tenth of a degree. The MULCON trajectory model produces an excellent approximation to an integrated trajectory.

V. Summary and Conclusions

As the results have shown, the techniques described in this paper is a very effective means of solving the multiple flyby trajectory optimization problem. Choosing the independent variables to be the physical parameters of interest leads to a convenient formulation by eliminating the need for penalty functions or nonlinear constraints in favor of simple range constraints on the independent variables. An attractive feature of the optimization procedure is that the minimum total ΔV solution can be found while retaining the advantages of a sum-of-squares cost function. One of the most important of these advantages is the use of a Newton optimization algorithm.

As shown in the results section and for many other satellite tours, most of the maneuver ΔV's become zero as might be expected from physical considerations. The remaining nonzero ΔV's are generally related to one or more of the flyby parameters which are at a limit. The maneuver times rarely have any significant effect upon the optimization, since apoapsis of the orbit around the central body is, in fact, usually the most efficient place to perform a small maneuver.

Appendix

The partial derivatives of the velocity discontinuities, $\Delta\bar{V}_i$, with respect to the independent variables, $\bar{P}_j$ and T_j, are given below. These partial derivatives are used in the computation of the gradient vector and the Hessian matrix.

$$\frac{\partial \Delta\bar{V}_i}{\partial \bar{P}_j} = \tag{A1}$$

$$\begin{cases} 0 & (0 \le i \le j-2) \\ U_j & (i=j-1) \\ (W_{j+1}B_j - D_j)U_j & (i=j) \\ (W_{j+2}ABW_{j+1} - CDW_{j+1})B_jU_j & (i=j+1) \\ (W_{i+1}ABW_i - CDW_i)\left(\prod_{k=j+1}^{i-1} ABW_k\right)B_jU_j & (j+2 \le i \le n-1) \end{cases}$$

$$\frac{\partial \Delta\bar{V}_i}{\partial T_j} = \tag{A2}$$

$$\begin{cases} 0 & (0 \le i \le j-1) \\ -W_{j+1}\Delta\bar{V}_j & (i=j) \\ -(W_{j+2}ABW_{j+1} - CDW_{j+1})\Delta\bar{V}_j & (i=j+1) \\ -(W_{i+1}ABW_i - CDW_i)\left(\prod_{k=j+1}^{i-1} ABW_k\right)\Delta\bar{V}_j & (j+2 \le i \le n-1) \end{cases}$$

where

$$ABW_i = A_i + B_iW_i \qquad CDW_i = C_i + D_iW_i \tag{A3}$$

$$\Phi(T_i, T_{i-1}) = \begin{bmatrix} A_i & B_i \\ C_i & D_i \end{bmatrix} \tag{A4}$$

§The integrated trajectory is generated by simple targeting from one maneuver point to the next, satisfying the times and positions at the maneuver points of the MULCON solution.

$\Phi(T_i, T_{i-1})$ is the state transition matrix of the ith trajectory segment from T_{i-1} to T_i.

$$W_i = \frac{\partial \bar{V}_{i-1}^{+}}{\partial \bar{R}_{i-1}}\Bigg|_{T_{i-1}, \bar{P}_i} \tag{A5}$$

where W_i gives the variation of the initial velocity on the ith trajectory segment with respect to the initial position when targeting from a fixed initial time to fixed flyby parameters.

$$U_i = \frac{\partial \bar{V}_{i-1}^{+}}{\partial \bar{P}_i}\Bigg|_{T_{i-1}, \bar{R}_{i-1}} \tag{A6}$$

where U_i gives the variation of the initial velocity on the ith trajectory segment with respect to the flyby parameters when targeting from a fixed initial time and position.

Acknowledgments

The authors would like to thank N.D. Hulkower for his contribution in developing trajectory generation software and W. Murray of Stanford University for his helpful suggestions with regard to the optimization procedure. The research described in this paper was carried out at the Jet Propulsion Laboratory, California Institute of Technology, under NASA Contract NAS7-100.

References

[1] McKinley, E.L., Jones, J.B., and Bantell, M.H. Jr., "Mariner Venus/Mercury 1973 Navigation Strategy," AAS/AIAA Astrodynamics Conference, Vail, Colo., July 1973.

[2] Kohlhase, C.E. and Penzo, P.A., "Voyager Mission Description," *Space Science Reviews,* Vol. 21, No. 2, Nov. 1977, pp. 77-101.

[3] Nock, K.T., "Interplanetary Trajectory Options for Project Galileo," AIAA Paper 80-1697, AIAA/AAS Astrodynamics Conference, Danvers, Mass., Aug. 1980.

[4] Diehl, R.E. and Nock, K.T., "Galileo Jupiter Encounter and Satellite Tour Trajectory Design," AAS Paper 79-141, AAS/AIAA Astrodynamics Conference, Provincetown, Mass., June 1979.

[5] Roberts, P.H. and Wright, J.L., "The Saturn Orbiter Dual Probe Mission Concept," AAS Paper 79-143, AAS/AIAA Astrodynamics Conference, Provincetown, Mass., June 1979.

[6] Farquhar, R.W. and Dunham, D.W., "A New Trajectory Concept for Exploring the Earth's Geomagnetic Tail," AIAA Paper 80-0112, AIAA Aerospace Sciences Meeting, Pasadena, Calif., Jan. 1980.

[7] D'Amario, L.A., Byrnes, D.V., Sackett, L.L., and Stanford, R.H., "Optimization of Multiple Flyby Trajectories," AAS Paper 79-162, AAS/AIAA Astrodynamics Conference, Provincetown, Mass., June 1979.

[8] Gill, P.E. and Murray, W., *Numerical Methods for Constrained Optimization,* Academic Press, New York, 1974, pp. 29-66.

[9] Byrnes, D.V., "Applications of the Pseudostate Theory to the Three-Body Lambert Problem," AAS Paper 79-163, AAS/AIAA Astrodynamics Conference, Provincetown, Mass., June 1979.

[10] Wilson, S.W., "A Pseudostate Theory for the Approximation of Three-Body Trajectories," AIAA Paper 70-1061, AIAA Astrodynamics Conference, Santa Barbara, Calif., Aug. 1970.

[11] Kwok, J.H. and Nacozy, P.E., "Final Report: Jet Propulsion Laboratory Contract #955140 and Updated User's Guide for MULCON," University of Texas at Austin, Austin, Tex., Jan. 1979.

[12] Stumpff, K. and Weiss, E.H., "Applications of an N-Body Reference Orbit," *Journal of the Astronautical Sciences,* Vol. XV, No. 5, Sept.-Oct. 1968, pp. 257-261.

[13] Byrnes, D.V. and Hooper, H.L., "Multi-Conic: A Fast and Accurate Method of Computing Space Flight Trajectories," AIAA Paper 70-1062, AIAA Astrodynamics Conference, Santa Barbara, Calif., Aug. 1970.

[14] D'Amario, L.A., "Minimum Impulse Three Body Trajectories," Ph.D. Dissertation, Massachusetts Institute of Technology, Cambridge, Mass., June 1973.